Plasma distribution models in a rotating magnetic dipole and refilling of plasmaspheric flux tubes

J. Lemaire
Institut d'Aeronomie Spatiale de Belgique, 3 Avenue Circulaire, B-1180 Bruxelles, Belgium

(Received 30 September 1987; accepted 9 February 1989)

Rotating stars or planets like Earth are sometimes surrounded by a dipolar magnetic field distribution. The thermal plasma forming a corona or an ionosphere around these astrophysical objects diffuses upward along the magnetic field lines and forms a toroidal region filled with this thermal plasma, like the terrestrial plasmasphere. The field-aligned distribution of this thermal ionospheric plasma is controlled by the gravitational and pseudocentrifugal potential distribution. One can distinguish two extreme types of plasma distribution in this field-aligned potential: the diffusive equilibrium distribution and the exospheric equilibrium distribution corresponding, respectively, (i) to a saturated, and (ii) to an almost depleted, magnetic flux tube. As a result of pitch angle scattering by Coulomb collisions, an increasing number of ions escaping from the ionosphere are stored in trapped orbits. These trapped particles have magnetic mirror points at high altitudes, i.e., in the low-density exospheric region. Also as a result of collisions, the field-aligned density distributions irreversibly evolve from exospheric equilibrium with a highly anisotropic pitch angle (cigarlike) distribution to a diffusive equilibrium distribution characterized by an isotropic pitch angle distribution. It is shown that the suprathermal ions become anisotropic much more slowly than ions of energies smaller than 1 eV.

I. INTRODUCTION

Rotating stars or planets like Earth are sometimes surrounded by a dipolar magnetic field distribution. The thermal plasma forming a hot corona or an ionosphere around these astrophysical objects diffuses upward along the magnetic field lines and forms a toroidal region filled with this thermal plasma, like the terrestrial plasmasphere. The plasmasphere is filled with cold plasma of ionospheric origin. This plasma has been produced in the ionosphere by photoionization and eventually escapes from the topside ionosphere into the protonosphere and magnetosphere along dipole magnetic field lines.

Although the following can be applicable to other stellar and planetary magnetospheres, for instance, that of Jupiter, this paper is specifically addressed to the case of Earth.

Only on rare occasions will the field-aligned distribution of plasma be stationary and in hydrostatic equilibrium. On such rare occasions, the field-aligned bulk velocity of the plasma is equal to zero. Hydrostatic equilibrium is an exceptional situation because of ever present north–south asymmetries of the geomagnetic field lines in the nonrotating frame of reference, as well as because of dissimilar boundary conditions in the conjugate ionospheres at the feet of magnetic flux tubes. Nevertheless, to start with simple cases, let us consider the cold plasma distribution in a convecting flux tube under the condition of hydrostatic equilibrium, i.e., when there is no net mass flow in any direction along the magnetic field direction.

II. FIELD-ALIGNED POTENTIAL AND THE DIFFERENT CLASSES OF PARTICLES

When hydrostatic equilibrium is satisfied, the plasma density decreases exponentially with altitude from a maximum value of the order of 10^6 cm^{-3} at the altitude of the F region (300 km) to a value of the order of 300 cm^{-3} in the equatorial plane at $L = 4$. The vertical density gradient is characterized by a scale height that is inversely proportional to the gravitational force: $H = k(T_i + T_e)/mg$. Note that it is the projection of the gravitational force along the local magnetic field direction which determines the actual field-aligned density scale height ($H_{//}$). This field-aligned component of the gravitational force depends, therefore, on the dip angle, which is a function of latitude along the field line.

Since we are in a rotating frame of reference which is accelerated, the pseudocentrifugal force that each particle experiences in addition to the gravitational force also has a projection along the direction of **B** as pointed out in an early study by Angerami and Thomas[1] as well as Eviatar *et al.*[2] The field-aligned component of the sum of the gravitational and centrifugal forces can be derived from a generalized potential ϕ_g that is given by

$$\phi_g(r,\lambda) = -GM_E/r - \tfrac{1}{2}\Omega^2 r^2 \cos^2\lambda + \text{const}, \qquad (1)$$

where Ω is the local angular velocity of the plasma, G is the gravitational constant, M_E is the mass of Earth, r is the radial distance, and λ is the dipole latitude.

It should be pointed out here that an ambipolar diffusion electric field builds up in plasmas as a result of long-range Coulomb interactions between charged particles, i.e., over distances larger than the Debye length. This electric field results from the charge separation of the ions and electrons in the gravitational and pseudocentrifugal field because of their different masses. In a plasma in hydrostatic equilibrium, this charge separation electric field is also known as the Pannekoek–Rosseland electric field.[3–5].

This ambipolar electric field has a component parallel to the magnetic field direction. The charge separation electric

 0899-8221/89/071519-07$01.90

field intensity $E_{//}$, is such that the sum of the electric, gravitational, and centrifugal forces is identical for the ions of mass m_i and for the electrons which have a much lower mass m_e: $eE_{//} + m_i \nabla_{//} \phi_g = -eE_{//} + m_e \nabla_{//} \phi_g$. Without this electric field the plasma could not be quasineutral.

Note that the total field-aligned potential associated with this Pannekoek-Rosseland electric field is generally less than 1 V. This is minuscule compared to the electric potential of 50–100 kV generated into the magnetosphere by $\mathbf{v} \times \mathbf{B}$ convection or simply by corotation of magnetospheric plasma with the Earth ionosphere. However we should remind the reader that the former potential difference is *along* magnetic field lines, while the latter is *perpendicular* to them. The large convection electric field perpendicular to the magnetic field depends on the frame of reference where it is measured: In a frame of reference comoving with the plasma velocity $v_\perp$ this "large" convection electric field is exactly equal to zero, but the field-aligned component of the ambipolar electric field does not vanish in the comoving frame of reference used in the rest of this paper. Indeed, the Lorentz transformation does not change the intensity of the electric field component parallel to the magnetic field direction. The frame of reference used in this paper is the corotating one, i.e., where the convection electric field is precisely equal to zero.

Taking into account the ambipolar diffusion electric field in a hydrostatic and rotating ion-exosphere, it can be shown that the difference of potential energy for a proton or electron between two points of latitude λ_0 and λ located along the field line L is given in eV by

$$\Delta\psi = -\frac{0.324}{L}\left[\frac{1}{\cos^2\lambda} - \frac{1}{\cos^2\lambda_0} + \frac{1}{3}\left(\frac{\Omega}{\Omega_E}\right)^2\left(\frac{L}{L_c}\right)^3 (\cos^6\lambda - \cos^6\lambda_0)\right], \quad (2)$$

where Ω_E is the angular speed of Earth (see also Refs. 6 and 7).

Figure 1 shows the value of $\Delta\psi$ as a function of latitude along five different field lines for $\Omega = \Omega_E$. Along the innermost magnetic field lines ($L = 2$, 3, or < 5.78) the total potential energy is an increasing function of altitude (solid lines). Along these field lines the ion density and electron density are decreasing functions of altitude with minimums in the equatorial plane. However, for the field lines at $L > 5.78$, $\Delta\psi$ has a minimum in the equatorial plane and two conjugate maxima at nonzero latitudes. The points where ψ is maximum are those where the magnetic field line crosses the so-called zero parallel force (ZPF) surface whose cross section is shown in Fig. 2. These points correspond to the places where the parallel component of $\mathbf{g}$ is balanced by the parallel component of the centrifugal force. Beyond this ZPF surface, the field-aligned component of the total force is directed outward, while inside this surface, closer to Earth, the gravitational force dominates the centrifugal force.

Very low energy (< 2 eV) charged particles spiraling along magnetic field lines are most sensitive to these gravitational, centrifugal, and electrical forces. Their trajectories in the total potential field depend on their kinetic energy ($\frac{1}{2}mv^2$) and pitch angle θ. Different classes of particles have been identified. In panel A of Fig. 2, the cross section of the

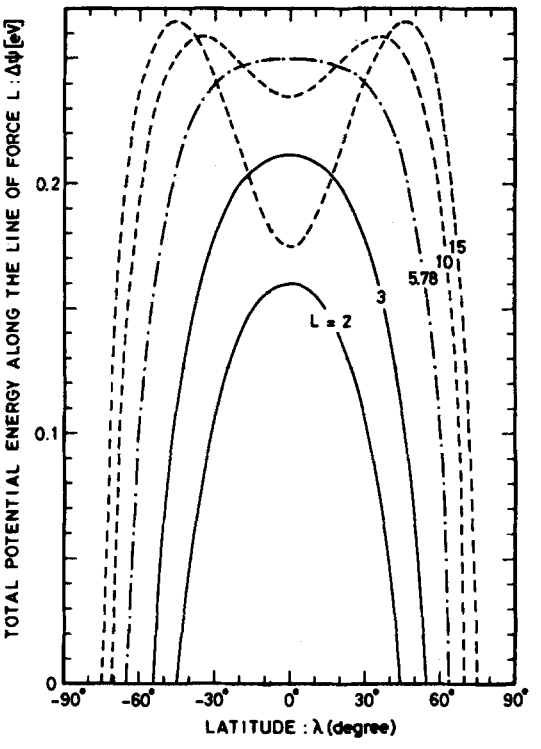

FIG. 1. Gravitational plus rotational potential energy of H^+ ions along different magnetic field lines corotating with Earth. For $L \leq 5.78$, the total potential $\Delta\psi$ has maximum value in the equatorial plane at $\lambda = 0$; for $L > 5.78$, $\Delta\psi$ has a minimum at the equator and two symmetrical maxima outside of the equatorial plane at $\lambda = \lambda_m$ (see Ref. 7).

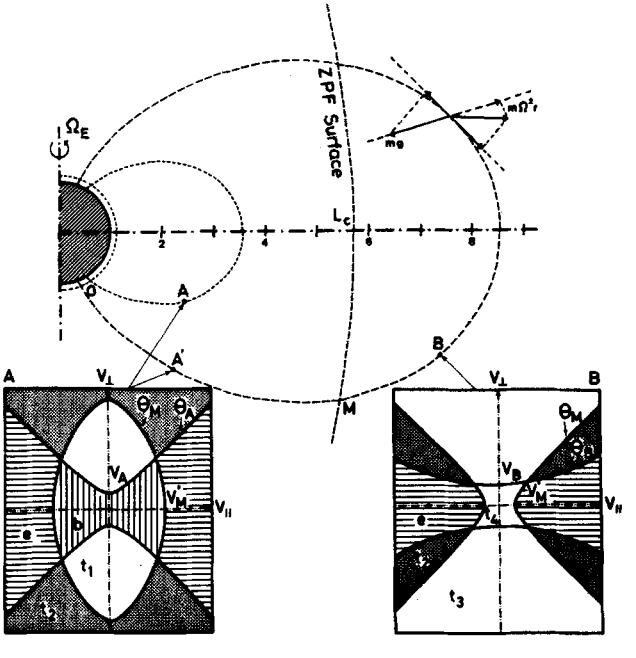

FIG. 2. Two dipole magnetic field lines: $L = 3.5$ and $L = 8.5$. The meridional cross sections of the zero parallel force (ZPF) surface where the field-aligned component of the gravitational and centrifugal force are equal. Here L_c is the equatorial distance of the ZPF surface; $L_c = 5.78$ for an ion-exosphere corotating with the angular speed of the Earth (Ω_E). The two panels with shaded areas show the different regions in velocity space corresponding to the different classes of charged particles below the ZPF surface at A and A', and above the ZPF surface at B. Particles with velocity components $v_{//}$ and $v_\perp$ inside the shaded areas labeled e, t_1–t_4, and b are, respectively, escaping, trapped, and ballistic particles (see Ref. 6).

velocity space ($v_{//}$,$v_{\perp}$) is shown. The different shadings correspond to different classes of orbits of particles.

Panel B shows the different classes of orbits of particles at a point B located beyond the ZPF surface. Ballistic particles represented by b correspond to those particles emerging from the ion-exobase (i.e., the 1000 km reference altitude level), which do not have enough kinetic energy to reach the equatorial plane; they fall back into the ionosphere in the same hemisphere. The escaping particles (represented by e) are those particles that have an energy larger than the potential barrier and that travel along the field line from the ion-exobase of one hemisphere to the conjugate region in the other hemisphere. In addition to these particles that emerge from the ionosphere, there are two classes of trapped particles (t_1, t_2) that have mirror points above the ion-exobase: t_2 corresponds to orbits with two magnetic mirror points in opposite hemispheres, while the t_1 trapped particles correspond to particles of low energy that have reflection points in the same hemisphere, the lower one being a magnetic mirror point while the upper one is a gravitational reflection point. It can be seen that beyond the zero parallel force surface (panel B) there are two new classes of trapped particles (t_3,t_4) corresponding to particles that are, respectively, magnetically and energetically trapped beyond the zero parallel force surface.

III. FIELD-ALIGNED DENSITY DISTRIBUTION AND FLUX TUBE REFILLING

The field-aligned density distribution, given by the upper solid line in Fig. 3, is obtained when all these possible orbits are populated with particles whose velocity distribution is an isotropic Maxwellian with a temperature independent of altitude. This field-aligned plasma distribution corresponds to barometric equilibrium or diffusive equilibrium (DE). The different shadings in this figure show the relative abundance of the different classes of particles as a function of latitude along the dipole field line $L = 8$. Note that in a nonrotating ion-exosphere, like that considered by Eviatar *et al.*,[2] there are no trapped particles of type t_3, t_4. Indeed, for a nonrotating ion-exosphere there is no potential well near the equatorial plane along any magnetic field line: The ZPF force surface is located at infinite radial distance when Ω tends to zero.

Let us consider a depleted magnetic flux tube and calculate t_N, the characteristic time necessary to recover the total flux tube content corresponding to diffusive equilibrium when the upward ionization flux is constant and equal to maximum polar wind evaporation flux.[7] The expression for t_N is briefly described in the Appendix. The values of this flux tube refilling time are given in Table I for a series of L values.

From Table I it can be seen that an empty flux tube at $L = 8$ would need at least 66 days before the state of diffusive equilibrium could be reached via particle evaporation from the ionosphere with a limiting polar wind flux (see lines 1 and 2 in Table I).

Whistler observations[8,9] indicate that flux tubes beyond $L = 4$ indeed refill very slowly: more than 5 days are required to saturate flux tubes that have L values larger than 4.

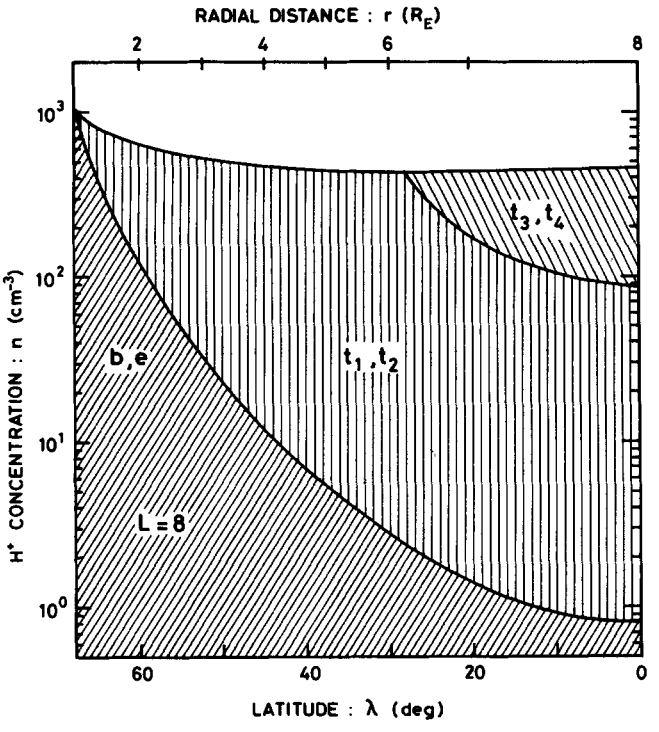

FIG. 3. Hydrogen plasma density distributions as a function of latitude (λ) along the dipole magnetic field line $L = 8$. The upper solid line corresponds to the diffusive equilibrium (DE) model for $N_0 = 10^3$ cm^{-3} and $T_0 = 3000$ K at the reference level altitude $h_0 = 1000$ km. The lower solid line represents the exospheric equilibrium (EE) kinetic model for symmetrical boundary conditions in both hemispheres. For both cases the ion-exosphere corotates with the angular velocity of Earth. The DE density has a minimum value at the latitudes $\lambda_m = \pm 27°$ and radial distance $r_m = 6.27$, where the magnetic field line penetrates through the ZPF surface. Note the large density contributed by trapped particles to the DE distribution.

This means that the flux tube at $L = 8$ will almost never reach the level of diffusive equilibrium before it experiences the next depletion at the onset of the next magnetic substorm. This also means that magnetic flux tubes for $L > 4$ will have a density that is generally smaller than the diffusive

TABLE I. Here t_N is the flux tube refilling time for different values of L. A limiting polar wind flux of 2×10^8 cm^{-2} is assumed to flow at a constant rate to increase the total flux tube content from the minimum exospheric equilibrium (EE) value of the maximum diffusive equlibrium (DE) value; t_F is the free-flight time of a thermal proton spiraling along the magnetic field line (L) from an altitude of 1000 km up to the equatorial plane. The proton has an energy of 0.25 eV ($T_0 = 3000$ K) and an initial pitch angle of 45° at 1000 km altitude; its field-aligned velocity is calculated along the field line assuming conservation of the magnetic moment of the particle and conservation of the sum of kinetic energy and potential energy illustrated in Fig. 1. Here t_S is the Coulomb collision time for momentum transfer of a thermal proton (0.25 eV, $T \simeq 3000$ K) gyrating in the equatorial plane. The background plasma density is assumed to be equal to that of the minimum exospheric equlibirum model (n_{eq}^{EE}).

L	2	4	6	8	R_E
t_N	9.4	115	544	1587	hours
t_N	...	4.7	22.7	66.1	days
t_F	0.7	1.9	3.6	5.2	hours
t_S	0.26	2.8	10	28	hours
n_{eq}^{EE}	80	8.1	2.2	0.82	cm^{-3}

equilibrium value given by the upper solid line in Fig. 3 for $L = 8$.

At the onset of a substorm, the plasmasphere is peeled off; all flux tubes located beyond some minimum equatorial distance are then depleted. Assuming that the density then becomes almost equal to zero everywhere within the flux tube, we may ask the question: How does the flux tube refill again? Or, how is the field-aligned plasma distribution evolving during the replenishment phase?

From a simple kinetic point of view, it can be considered that ballistic and escaping particles (b and e classes of particles) will immediately invade the empty flux tube and build up a density distribution corresponding to an exospheric equilibrium (EE). All this can be achieved in about 1–5 h of time. This time delay represents the characteristic time of free flight (t_F) for a thermal ion with an energy equal to $3kT_0/2$ and moving along the flux tube at $L = 8$ from the 1000 km altitude level up to the equatorial plane. It is defined in the Appendix. The values of t_F are given in line 4 of Table I for different values of L.

The exospheric equilibrium density is shown by the lower solid line in Fig. 3. Only ballistic and escaping particles are present in this extreme case; the velocity distribution is almost empty at the largest pitch angles corresponding to trapped particles t_1, t_2, t_3, and t_4. The pitch angle distribution is then strongly field aligned and almost confined in the source cone ($0 < \theta < \theta_B$) and in the loss cone ($\pi - \theta_B < \theta < \pi$) (see Fig. 2). At large pitch angles corresponding to trapped particles there should be no (or almost no) particles during the first 1–5 h. However, since the binary Coulomb collision frequency is not strictly equal to zero, but increases continuously while the flux tube is refilling, one can expect that higher densities are building up exponentially by continuous addition and piling up of particles on trapped orbits. Indeed, although relatively rare in the plasmasphere, Coulomb collisions are, however, frequent enough to scatter escaping and ballistic particles on orbits with larger pitch angles (see line 5 in Table I).

Note that interactions of particles with ion acoustic waves generated by unstable counterstreaming ion flows may produce additional trapping of escaping and ballistic ions.[10] Once deflected on trapped orbits at higher altitudes where the density is lowest, these particles have a lower collision probability and, consequently, they have a tendency to stay and accumulate there. As a result of these irreversible trapping mechanisms, the ambient plasma density increases continuously until eventually, after a period of several days, the flux tubes reach the state of diffusive equilibrium illustrated by the upper curve in Fig. 3 for $L = 8$.

According to the refilling scenario presented above, the field-aligned density distribution would evolve from a minimum exospheric equilibrium to a maximum diffusive equilibrium density distribution.

Other scenarios for the refilling of magnetic flux tubes have been proposed.[11–18] These are based on the assumption that hydrodynamic shock fronts propagate from the ionosphere up to the equatorial plane or backward. According to these time-dependent hydrodynamic descriptions, the whole flux tube should be refilled in a few hours time. Observations, however, indicate that the refilling process takes place over several days.[8,9] These alternative scenarios based on propagating hydrodynamic shocks are much faster processes than refilling by diffusion and kinetic evaporation, which takes more than 5 days for magnetic flux tubes located beyond $L = 4$. Consequently, the slow refilling rates observed by Parks[8] support the latter mechanism, i.e., the kinetic evaporation.

IV. PITCH ANGLE SCATTERING BY COULOMB COLLISIONS

It is important not to underestimate the role played by Coulomb collisions as an efficient pitch angle scattering mechanism for thermal and suprathermal ions. At the beginning of the refilling process the ion pitch angle distribution should be mainly field aligned and confined within the source cone; however, as time passes, the ambient plasma density increases and, consequently, more and more particles will be scattered in trapped orbits. It should also be noted that the fastest particles (the most energetic forerunners, i.e., the suprathermal ions) forming the tail of the Maxwellian velocity distribution remain anisotropic and field aligned longer than the ions with lower energies. Indeed, the Coulomb collision cross section for momentum transfer decreases rapidly with the energy of the incident charged particles. Therefore we expect the pitch angle distribution of particles with the lowest energies to become isotropic first. It is only after a longer period of time that the pitch angles of suprathermal particles tend also to become isotropic, i.e., when the cold background density has increased to a relatively high value.

The slowing down Coulomb collision time (t_S) (i.e., for the momentum transfer) of a thermal proton (0.25 eV, $T = 3000$ K) gyrating in the equatorial plane is given in line 5 of Table I for the case when the background plasma is in exospheric equilibrium (see the Appendix for a definition of t_S). It can be seen that at $L = 4$ in the equatorial plane a thermal proton of 0.25 eV can remain trapped without having a significant pitch angle deflection for almost 3 h. At $L = 8$ the collision time t_S is ten times longer. These values have been calculated for the minimum equatorial density corresponding to the exospheric equilibrium.

During the process of refilling, the density approaches the diffusive equilibrium value, and the Coulomb collision time t_S is then gradually reduced by a larger and larger factor. For example, the diffusive equilibrium density is 60 times larger at $L = 4$ than the exospheric equilibrium density: therefore, t_S is 60 times smaller ($t_S = 2.8$ min) than the value given in Table I for the case of exospheric equilibrium.

When the equatorial density is 0.8 cm^{-3} at $L = 8$ (corresponding to exospheric equilibrium), t_S is larger than 1 day; when diffusive equilibrium is achieved along this field line, the equatorial density is more than two orders of magnitude larger and, consequently, t_S is two orders of magnitude smaller.

These estimates show that within the plasmasphere where the density is high, Coulomb collisions play an important role up to the equatorial region. Field-aligned beams of

ions cannot survive very long, unless these beams are formed of suprathermal particles whose binary Coulomb collision cross section is significantly smaller than that of the very low energy thermal ions.

However, outside the plasmasphere and in the polar wind where the density is lower (i.e., closer to exospheric equilibrium), anisotropic velocity distributions of thermal ions are expected to survive for a much longer period of time, even at energies as low as 1–2 eV. This is indeed the case according to observations of Dynamic Explorer 1.[19–22]

Table II gives the number of Coulomb collisions (q) for protons and electrons injected at 1000 km altitude with an initial pitch angle θ_0 and an initial velocity v_0, i.e., an initial energy $K_0 = \frac{1}{2}mv_0^2$; q_1 is the expected number of collisions for a background plasma density distribution in diffusive equilibrium assuming that the field particles have a temperature of 3000 K and a density of 10^3 cm^{-3} at 1000 km altitude; q_2 is the expected number of collisions when the background density distribution is in exospheric equilibrium for the same exobase conditions (see Ref. 7 and the Appendix for the definition of q). Also given in this table is the free-flight time (t_F) of the particle from the 1000 km level up to the equatorial plane.

It can be seen that thermal protons or electrons experience several collisions during their upward motion toward the equatorial plane. When the field particle density corresponds to diffusive equilibrium, the expected number of collisions (q_1) is almost ten times larger than for exospheric equilibrium (q_2). For suprathermal energies ($K_0 = 26$ eV $v_0/v_T = 10$, where v_T is the thermal speed of the field particles and v_0 the velocity of the test particle at 1,000 km) the values of q_1 and q_2 decrease rapidly below unity. This drastic reduction results from the sensitivity of the Coulomb collision cross section on the energy of the incident test particle. Therefore it can again be concluded that large departures from isotropic pitch angle distributions are expected for suprathermal protons with energies larger than 5–10 eV. Note also from Table II that protons are more effectively deflected by binary close Coulomb collisions with field protons than with field electrons. A test electron is much more efficiently scattered by field electrons than by field protons of the same mean energy.

The electrons make their way to the equatorial plane 43 times faster than the protons of the same energy (t_F is given in Table II), but electrons experience almost the same number of collisions as protons. Therefore it can be concluded that Coulomb collisions will restore isotropy of electron velocity distribution 43 times faster than thermal ions upwelling from the ionosphere.

It can also be shown that the number of Coulomb collisions q_2 in an exospheric equilibrium model is almost independent of L, i.e., independent of the length of the magnetic field line. Indeed, in exospheric equilibrium, the background density decreases very rapidly with r, i.e., almost as r^{-4} (see Ref.6). The lengthening of the magnetic field line with L does not contribute much to increase q_2 because along the additional field line length the background density is indeed very small. On the contrary, when the background density distribution is in diffusive equilibrium, the expected number of collisions (q_1) is almost two times larger along $L = 8$ than along $L = 4$. The free-flight time (t_F) is a factor 2.8 larger at $L = 8$ than at $L = 4$.

As a matter of consequence, plasma with energy below 1 eV is collision dominated inside the plasmasphere where the density is high. Its field-aligned distribution can therefore be modeled satisfactorily in the framework of standard hydrodynamic approximations which are applicable to collision-dominated plasmas. Chapman–Enskog's expansions for the velocity distributions are then expected to be valid and satisfactory approximations. Expressions for the transport coefficients (diffusion, viscosity, heat conduction,...) can then be approximated by their standard expressions based on the assumptions that the departures from Maxwellian velocity distribution are only small first-order corrections (for a comprehensive review see Ref. 23).

However, a correct description of the suprathermal ions inside the plasmasphere requires a proper kinetic treatment based on Boltzmann's equation including the scattering effects by Coulomb interactions, as emphasized by Fahr and Shizgal[24] and Shizgal *et al.*[25]

TABLE II. Expected number of Coulomb collisions for protons (p^+) and electrons (e^-) injected at 1000 km with a pitch angle (θ_0), an initial velocity (v_0), i.e., an initial energy K_0; q_1 is the expected number of collisions for a background plasma density distribution in diffusive equilibrium ($T_F = 3000$ K and $n_F = 10^3$ cm^{-3} at 1000 km, $v_T^2 = 2kT_F/m$); q_2 is the expected number of collisions when the background density distribution is in exospheric equilibrium for the same exobase conditions; and t_F is the free-flight time of the test particle from the 1000 km level up to the equatorial plane along the field line $L = 4$.

Test particle	Field particle	v_T/v_0	K_0 (eV)	θ_0 (deg)	q_1	q_2	t_F (sec)
p	p	1	0.26	45	55.0	6.7	6790
p	p	1	0.26	0	52.0	5.8	6450
p	e	1	0.26	45	35.3	4.9	6790
p	p	1.5	0.58	45	13.5	2.0	3190
p	p	3.0	2.33	45	0.81	0.13	1410
p	p	10	25.8	45	0.0059	0.001	409
e	p	1	0.26	45	5.15	0.36	159
e	p	1.5	0.58	45	0.24	0.032	74
e	p	3.0	2.33	45	0.0095	0.0016	33
e	p	10	25.8	45	0.0000 68	0.0000 12	9.5
e	e	1	0.26	45	55.0	6.7	159

Whether additional pitch angle scattering of these warm ions by wave–particle interactions is required is not yet established and depends on the spectral range and intensity of the waves with which these particles can resonate. Therefore, instead of speculating on the possible importance of such wave–particle interactions, we suggest concentrating our efforts, first, on kinetic effects due to straightforward Coulomb collisions and, subsequently, to evaluate what remains to be explained by other alternative irreversible processes.

V. CONCLUSIONS

In the first part of this paper we have described two extreme models of the rotating ion-exosphere of Earth, in order to evaluate the importance of Coulomb collisions on exospheric plasma velocity distributions. The first model considered corresponds to diffusive equilibrium (DE). This model belongs to the class of hydrodynamical models, since it is based on the assumption that the collision frequency is large enough to maintain a Maxwellian and isotropic velocity distribution for particles of all energies. This type of model gives appropriate descriptions of the densest part of the inner terrestrial plasmasphere as well as of the topside ionosphere of other planets or stars with a dipolar magnetic field distribution. Indeed, in these dense regions the mean-free path (ℓ) of the thermal particles forming the bulk of the velocity distribution is smaller than the plasma density scale height H. From Table II it has been deduced that protons and electrons with energies below 1 eV indeed have a large number of collisions before they can reach the equatorial plane. Furthermore, for these thermal particles ℓ is, indeed, also much smaller than LR_E, the characteristic length of the magnetic field lines.

In the outer part of the plasmasphere, where magnetic flux tubes are often significantly depleted, ℓ is larger than H above a certain altitude. Hydrodynamical approximations therefore fail to be applicable above this altitude.

The second type of model considered above were those corresponding to exospheric equilibrium (EE). They belong to the class of zeroth-order kinetic models for which the mean-free-path ℓ of all particles is not only assumed to be larger than H but also much larger than LR_E.

This exospheric equilibrium model gives an extremely low field-aligned plasma density distribution which possibly may prevail soon after plasmaspheric flux tubes have been depleted at the onset of a large magnetic substorm.[9]

The refilling process of such depleted flux tubes has been qualitatively described here in terms of Coulomb pitch angle scattering of ballistic and escaping particles emerging from the topside ionosphere. The consequence of these nonlocal Coulomb interactions occurring in the tenuous exosphere is to increase gradually and irreversibly the relative population of trapped particles that have mirror points at high altitudes. This kinetic refilling of magnetic flux tubes takes a rather long time (5 days for a flux tube at $L = 4$) but it fits well the results obtained from whistler observations.[8] This kinetic refilling mechanism is an alternative to the much faster hydrodynamic shock wave propagation models that are not supported by observations.

Although the zeroth-order kinetic models are useful and appealing because of their simplicity and because they give zeroth-order approximations for the field-aligned densities, these exospheric equilibrium models, however, need to be improved sooner or later and replaced by more accurate solutions of Boltzmann's equation, including the Coulomb collision operator.

This second generation of kinetic models will also be welcome to describe properly the energy and pitch angle distribution of the suprathermal ions observed in and outside the plasmasphere. Indeed, as can be seen from Table II, their mean-free path depends very much on their energy in the range 1–10 eV.

APPENDIX: CHARACTERISTIC REFILLING TIMES t_N; FREE-FLIGHT TIMES t_F; COLLISION TIMES t_S; NUMBER OF COLLISIONS q

1. Characteristic refilling times t_N

If F is the constant ionization flux escaping out of the topside ionosphere through a unit surface (S_0), the characteristic time (t_N) necessary to refill an empty flux tube to recover the total flux tube particle content (N_T^{DE}) corresponding to diffusive equilibrium is given by

$$t_N = N_T^{DE} F S_0. \tag{A1}$$

The maximum upward ionization flux is of the order of the free evaporation flux at the exobase where the mean-free path of the ions becomes equal to the plasma density scale height. This maximum upwelling flux is equal to

$$F = \tfrac{1}{4} n_0 (8kT_0/\pi m_H)^{1/2} \tag{A2}$$

(see Ref. 26), where m_H is the ion mass and n_0 and T_0 are, respectively, the density and temperature at the exobase. Assuming that $n_0 = 1000\ \text{cm}^{-3}$ and $T_0 = 3000$ K, we have $F = 2\times 10^8\ \text{cm}^{-2}\ \text{s}^{-1}$. The value of N_T^{DE} is a function of L. For $L = 4$, $N_T^{DE}/S_0 = 8.4\times 10^{13}$ protons/cm^2, we obtain $t_N > 115$ h (see Ref. 7).

2. Free-flight times t_F

The lapse time necessary for a thermal proton to spiral along a magnetic field line from the ionosphere up to the equatorial plane is defined as

$$t_F = \int_{1000\ \text{km}}^{\text{equator}} \frac{dl}{v_{\parallel}}, \tag{A3}$$

where $v_{//}$ is the component of the velocity parallel to the magnetic field direction. For a proton with an initial pitch angle of 45° at 1000 km altitude and an initial velocity equal to the mean thermal speed of protons at 3000 K, the values of t_F are given in Table I for different L-values. (from Ref. 7).

3. Collision time t_N

The mean Coulomb collision time for a thermal proton gyrating in the equatorial plane with a pitch angle of 90° is given by

$$t_S = 0.5 T^{3/2}/n\ (\text{sec}), \tag{A4}$$

where T and n are the temperature (in K) and density (in cm^{-3}) of the background hydrogen plasma. The values of t_S

are given in Table I for different L values and for different equatorial densities (taken from Ref.7).

4. Total number of collisions q

A thermal proton escaping at the altitude of 1000 km from the upper ionosphere usually experiences more than one 90° pitch angle deflection before it can reach the equatorial plane. The expected number of collisions of a particle spiraling along a field line L is defined by

$$q = \int_0^{t_F} \frac{dt}{t_c}, \tag{A5}$$

where t_F is the free-flight time defined above in Sec. 2; t_c is the characteristic Coulomb collision time; this collision time depends on the background proton density n_B along the magnetic field line L; and t_c also is a complicated function of the energy of the test particle given in classical text books on plasma physics like that of Spitzer.[27]

Integration over time, dt, is replaced by integration over dl, the length of the field line L: $dt = dl/v_{//}$.

In the calculation of q the value of $v_{//}$ is, as n_B, a function of the position along the magnetic field. Therefore, q depends on the initial pitch angle θ_0 and on the model used for the field-aligned density distribution of the background particles.

The expressions for q_1 and q_2, corresponding, respectively, to diffusive equilibrium and exospheric equilibrium, have been calculated in Ref.7 and are given in Table II for different particle energies, pitch angles, θ_0, and L values.

[1] J. J. Angerami and J. O. Thomas, J. Geophys. Res. **69**, 4537 (1964).
[2] A. Eviatar, A. M. Lenchek, and S. F. Singer, Phys. Fluids **7**, 1775 (1964).
[3] A. Pannekoek, Bull. Astron. Inst. Neth. **19**, 107 (1922).
[4] M. P. Mange, J. Geophys. Res. **65**, 3833, (1960).
[5] S. Rosseland, Mon. Not. R. Astron. Soc. **84**, 720 (1924).
[6] J. Lemaire, Planet. Space Sci. **24**, 975 (1976).
[7] J. Lemaire, Aeronomica Acta A **298**, 263 (1985).
[8] C. G. Park, J. Geophys. Res. **75**, 4249 (1970).
[9] P. Corcuff, Y. Corcuff, D. L. Carpenter, C. R. Chappell, J. Vigneron, and N. Kleimenova, Ann. Geophys. **28**, 679 (1972).
[10] M. Schulz and H. C. Koons, J. Geophys. Res. **77**, 248 (1972).
[11] P. M. Banks, A. F. Nagy, and W. I. Axford, Planet. Space Sci. **19**, 1053, (1971).
[12] R. W. Schunk and D. S. Watkins, Planet. Space Sci. **27**, 433 (1979).
[13] N. Singh and R. W. Schunk, J. Geophys. Res. **87**, 9154 (1982).
[14] N. Singh and R. W. Schunk, J. Geophys. Res. **88**, 7867 (1983).
[15] N. Singh and R. W. Schunk, Phys. Fluids **26**, 1123 (1983).
[16] N. Singh and R. W. Schunk, J. Geophys. Res. **90**, 6487 (1985).
[17] T. I. Gombosi, T. E. Cravens, and A. F. Nagy, Geophys. Res. Lett. **12**, 167 (1985).
[18] U. Samir, K. H. Wright, Jr., and N. H. Stone, Rev. Geophys. Space Phys. **21**, 1631 (1983).
[19] J. J. Sojka, R. W. Schunk, J. F. E. Johnson, J. H. Waite, and C. R. Chappell, J. Geophys. Res. **88**, 7995 (1983).
[20] T. Nagai, J. H. Waite, Jr., J. L. Green, C. R. Chappell, R. C. Olsen, and R. H. Comfort, Geophys. Res. Lett. **11**, 669 (1984).
[21] J. L. Horwitz, C. R. Chappell, D. L. Reasoner, P. D. Craven, J. L. Green, and C. R. Baugher, in *Energetic Ion Composition in the Earth's Magnetosphere*, edited by R. G. Johnson (Terra Scientific, Tokyo, 1983), p.263.
[22] J. L. Horwitz, R. H. Comfort, and C. R. Chappell, Geophys. Res. Lett. **11**, 701, (1984).
[23] R. W. Schunk, Rev. Geophys. Space Phys. **15**, 429, (1977).
[24] H. J. Fahr and B. Shizgal, Rev. Geophys. Space Phys., **21**, 75, (1983).
[25] B. Shizgal, U. Weinert and J. Lemaire, in *Proceedings of the 15th International Symposium on Rarefied Gas Dynamics*, Grado (Teubner, Stuttgart, 1986), Vol. II, p. 374.
[26] J. Lemaire and M. Scherer, Space Sci. Rev. **15**, 591 (1974).
[27] L. Spitzer, Jr., *Physics of Fully Ionized Gases*, (Wiley–Interscience, New York, 1956), p. 105.